Ecological Modelling 274 (2014) 29–40

Contents lists available at ScienceDirect

Ecological Modelling

journal homepage: www.elsevier.com/locate/ecolmodel

Mechanistic modeling of seed dispersal by wind over hilly terrain

A. Trakhtenbrot[a,b,*], G.G. Katul[b], R. Nathan[a]

[a] Movement Ecology Laboratory, Department of Ecology, Evolution and Behavior, The Alexander Silberman Institute of Life Sciences, The Hebrew University of Jerusalem, Edmond J. Safra Campus, Jerusalem 91904, Israel

[b] Nicholas School of the Environment, Duke University, Box 90328, Durham, NC 27708, USA

A R T I C L E   I N F O

Article history:
Received 4 May 2013
Received in revised form
20 November 2013
Accepted 24 November 2013
Available online 20 December 2013

Keywords:
Seed dispersal by wind over non-flat topography
Mechanistic seed dispersal model
Landscape heterogeneity effects on seed vector movement
Anisotropic dispersal kernel
Coupled Eulerian–Lagrangian closure (CELC) approach
Connectivity

A B S T R A C T

Seed dispersal is the main movement mechanism used by plants. The last decade saw rapid progress in understanding the underlying processes, especially for dispersal by wind, in part due to new mechanistic modeling approaches that account for turbulent fluctuations. Yet, current wind dispersal models stop short of explicitly incorporating the effects of landscape topography on the main transporting vector – wind, so that the effects of wind variability over hills on dispersal patterns remain by and large unstudied.

A new mechanistic model was developed that combines Eulerian wind statistics derived from a simplified analytical approach of flow over gently sloped forested hills with a Lagrangian seed trajectory model. Model runs were used to explore the effects of seed release location along the hill on dispersal kernels predicted by the new model in relation to their flat-terrain counterparts. The model was parameterized for a *Pinus taeda* plantation, and a range of seed motion capacities represented by terminal velocity and release height, and realistic topographic variation were then explored.

To evaluate model performance, computed kernels were compared to kernel measurements collected in a large flume for spherical 'seeds' released near the top of a rod canopy covering gentle cosine hills. The evaluation showed that the model reproduced the key experimental differences in dispersal patterns for releases at the hill crest and bottom.

The simulations revealed several novel findings. For seeds released within the canopy, both median and 99th percentile dispersal distances on the hill upwind side were up to two times longer than on flat terrain for the same motion capacity. Seeds released on the lee side traveled mostly toward the hill crest – following the local within-the-canopy wind direction. This direction was contrary to the 'regional' wind direction set by the flow conditions above the canopy. There, the directionality of the long-distance dispersal was additionally dependent on uplifting probability, affected by seed motion capacity.

It was demonstrated that neglecting the effects of even gentle topography in mechanistic seed dispersal models can lead to biased estimates of dispersal distances and directionality on hilly terrain. These results are pertinent to plant population demography, connectivity and spread on hills. More broadly, the approach developed here can be extended to movement of pollen and various airborne organisms over hills.

1. Introduction

Seed dispersal, or the transport of seeds away from a parent plant, is the main movement mechanism in plants (Ridley, 1930; van der Pijl, 1982; Levin et al., 2003; Nathan et al., 2008b). As such, seed dispersal is central to a broad array of ecological processes. Short-distance dispersal (SDD) generates the spatial template for subsequent demographic processes (e.g. establishment) and plays a role in species coexistence. The inherently rare long-distance dispersal (LDD) is crucial for landscape-scale processes such as colonization of new sites or re-colonization after a local extinction, inter-population connectivity and gene flow, and community assembly from the metacommunity (Levine and Murrell, 2003; Trakhtenbrot et al., 2005; Nathan et al., 2008b).

On the individual and the population level, the spatio-temporal dispersal patterns result from the intricate interplay of the plant traits determining the seed dispersal ability (motion capacity *sensu* Nathan et al., 2008a) and the vector characteristics, such as its seed load (Nathan et al., 2008b; Cousens et al., 2008). In the transportation phase of the dispersal event, factors affecting the movement of the dispersal vector(s) are of the utmost importance

* Corresponding author at: Nicholas School of the Environment, Box 90328, Duke University, Durham, NC 27708, USA. Tel.: +1 919 613 8068; fax: +1 919 684 8741.
E-mail addresses: anna.trakhtenbrot@duke.edu, ana.trakhtenbrot@mail.huji.ac.il (A. Trakhtenbrot).

0304-3800/$ – see front matter
http://dx.doi.org/10.1016/j.ecolmodel.2013.11.029

(Nathan et al., 2008b). The movement of both biotic and abiotic vectors is well known to be affected by landscape heterogeneity (e.g. Mack, 1995; Levey et al., 2005, 2008; Belcher et al., 2012). Topography is a widespread heterogeneity defining natural landscapes. Yet, while the effects of topography on dispersal were previously studied on a wide range of spatial scales – from microtopographic effects on seed deposition (e.g. Reader and Buck, 1986) to the possible role of mountain ranges as dispersal barriers (e.g. Rupp et al., 2001; Gugger et al., 2008), only a few studies have examined mechanistically and systematically the effects of complex topography on the movement of seed dispersal vectors and on its consequences to dispersal distances and directionality. One exception is the Mack (1995) study showing that *Aglaia aff. flavida* seeds dispersed by dwarf cassowaries (*Casuarius bennetti*) were moved predominantly uphill, mainly due to cassowary-preferred resting sites on ridgetops and level bluffs; while seeds contained in fruit falling from the trees and not treated by cassowaries were deposited mainly downhill from the source due to gravity.

Studying the effects of topography on the movement of biotic dispersal vectors may be extremely challenging and species-specific, as exemplified by Mack (1995). On the other hand, since wind is a dispersal vector common to many species and ecosystems (Willson et al., 1990; Ozinga et al., 2004), and because wind dynamics can be predicted from physical principles, wind dispersal is a logical starting point to disentangle the possible effects of topography on seed dispersal kernels.

Significant effort was devoted to mechanistic treatment of wind mediated dispersal over the last decade (see review in Nathan et al., 2011b). Indeed, there is wide agreement (e.g. Cousens et al., 2010) that currently mechanistic modeling is more advanced for wind than for other dispersal vectors. Physical models provide insights on possible causal links between the movement of this vector and its interaction with environmental factors and the dispersal patterns (Nathan et al., 2001, 2002a,b; Tackenberg, 2003; Soons et al., 2004; Katul et al., 2005; Nathan and Katul, 2005; Nuttle and Haefner, 2005; Kuparinen et al., 2007; Bohrer et al., 2008; reviewed in Kuparinen, 2006 and in Nathan et al., 2011b). A major advancement in recent years was in incorporating into the mechanistic models some of the main features of turbulent vertical velocity fluctuations whose coherency and vertical gradients were shown to be necessary to the onset of LDD (Nathan et al., 2002b; Tackenberg, 2003; Soons et al., 2004; Kuparinen et al., 2007; Bohrer et al., 2008; Wright et al., 2008).

Hilly terrain changes the basic balance of forces driving wind flow as compared to flat terrain (Stull, 1988; Finnigan and Belcher, 2004). These fundamental differences are expected to alter seed dispersal kernels, yet have rarely been considered in present mechanistic models or in empirical studies. A recent laboratory study in a flume demonstrated that dispersal distances of heavy spherical particles released from the top of a rod canopy situated on top of a gentle cosine hill were considerably larger than their counterpart releases at the bottom of the hill for the same canopy (Katul and Poggi, 2012). Yet, most mechanistic models of seed dispersal by wind to date were developed for flat terrain with perhaps some exceptions (Tackenberg, 2003; Horn et al., 2012). In one previous effort, incorporating some effects of topography into mechanistic seed trajectory calculations was attempted (PAPPUS model, Tackenberg, 2003), though this treatment was primarily an alignment of the mean flow streamlines along the topography using a pre-defined angle between the mean flow and topography. Thus, a mean vertical velocity component, resulting from the inclination of the wind vector direction to follow the terrain, was added (in contrast to a mean zero vertical component on flat terrain). PAPPUS did not explicitly model or treat spatial (i.e. horizontal and vertical) variations in wind flow dynamics generated by non-flat topography.

The lack of mechanistic seed dispersal models by wind for hilly terrain is not surprising given that simplified theories for turbulent wind flow over a hill covered by a uniform vegetated canopy, as opposed to a bare hill (Jackson and Hunt, 1975), was only developed in the last decade (Finnigan and Belcher, 2004, reviewed in Belcher et al., 2008, 2012). Analytical models of flow over a gentle hill covered by uniformly vegetated canopy were tested in flumes and via Large Eddy Simulations (LES) runs for isolated and train of gentle hills (Finnigan and Belcher, 2004; Poggi and Katul, 2007a,b,c; Dupont et al., 2008; Poggi et al., 2008; Patton and Katul, 2009). Good agreement between analytical models and observed mean flow patterns was reported in several cases (Poggi et al., 2008) – at least for the case of gentle hills and dense yet tall canopies. The relative simplicity of these analytical approaches is advantageous for incorporating them into seed dispersal models, since they enable computing dispersal patterns over large temporal (up to yearly) and spatial (up to tens of kilometers) domains that are the most relevant for many ecological processes.

Building on these previous efforts, a model is constructed so as to examine, for the first time, the effects of topography-induced variability in wind dynamics on seed dispersal by wind, as referenced to the flat terrain scenario. Our main goal was proposing a model that enables both to test hypotheses about the topographically induced modifications of the dispersal patterns and, more importantly, to generate new hypotheses on dispersal patterns. Specifically, for SDD, our hypothesis was that variations in dispersal distances and direction across the hill will follow patterns of within-the-canopy mean terrain-following wind velocity established in vicinity of the release site. The complex interaction of the mean terrain-following and normal-to-terrain velocities and the turbulent wind parameters (both within and above the canopy) that governs LDD prevents formulation of specific hypotheses on LDD patterns. It follows that the model runs serve here to generate novel hypotheses on LDD in complex terrain and its potential role in inter-population connectivity in terms of dispersal directionality. It is envisaged that these new hypotheses and model runs will guide the planning of future field experiments intended to explore the role of topography on dispersal patterns.

2. Methods

2.1. Overview of wind flow over hills

The main factors affecting wind flow over a hill are the hill slope, surface roughness, and the atmospheric stability parameter, a dimensionless variable that dictates whether the flow is dominated by mechanical or by convectively produced turbulence (Stull, 1988; Finnigan and Belcher, 2004). The key features of a flow over a bare hill under a nearly neutral stability regime (where mechanically produced turbulence is dominant) are the acceleration of the mean terrain-following velocity component on the upwind side, and its deceleration on the lee side due to pressure gradients produced by the hill surface (Jackson and Hunt, 1975; Stull, 1988; Finnigan and Belcher, 2004; Poggi and Katul, 2007b). This spatial variability in the longitudinal dimension is in contrast with the planar-homogeneous mean horizontal velocity characterizing the flow over flat terrain with uniform vegetation cover. Canopy cover on a hill further complicates the flow regime by imposing additional drag opposing the flow in both longitudinal and vertical directions (Finnigan and Belcher, 2004).

In the presence of a uniform canopy cover, the main conservation equations for the mean air density ($\bar{\rho}$) and mean longitudinal momentum balance within the canopy are:

$$\frac{\partial \overline{\rho}}{\partial t}+\frac{\partial \overline{\rho U}}{\partial x}+\frac{\partial \overline{\rho W}}{\partial z}\approx\frac{\partial \overline{U}}{\partial x}+\frac{\partial \overline{W}}{\partial z}=0$$

$$\overbrace{\bar{U}\frac{\partial \bar{U}}{\partial x}+\bar{W}\frac{\partial \bar{U}}{\partial z}}^{T_1}=\underbrace{-\frac{1}{\bar{\rho}}\frac{\partial \bar{P}}{\partial x}}_{T_2}-\overbrace{\frac{\partial \overline{u'w'}}{\partial z}-\frac{\partial \overline{u'u'}}{\partial x}}^{T_3}-\underbrace{C_d a \bar{U}^2}_{T_4}, \quad (1)$$

where air flow is assumed to be incompressible so that $\partial\bar{\rho}/\partial t=0$, $\overline{U}$ and $\overline{W}$ are the mean longitudinal and vertical velocities in a terrain-following coordinate system defined by x and z, $\overline{P}$ is the mean pressure, $\overline{u'w'}$ and $\overline{u'u'}$ are the mean momentum flux and longitudinal velocity variance, C_d is a local foliage drag coefficient, and a is the leaf area density. Terms T_1, T_2, T_3, and T_4 mathematically represent the mean advective acceleration, the mean pressure gradient produced by topographic variation, the turbulent stress gradients (generally dominated by contributions from $\partial\overline{u'w'}/\partial z$), and the drag force exerted by the foliage on the flow, accordingly.

Upon invoking first-order closure principles for the turbulent stress,

$$\overline{u'w'}(x,z)=-l_m^2(z)\left|\frac{\partial \overline{U}}{\partial z}+\frac{\partial \overline{W}}{\partial x}\right|\left(\frac{\partial \overline{U}}{\partial z}+\frac{\partial \overline{W}}{\partial x}\right), \quad (2)$$

where l_m is the mixing length, assumed to be constant inside the canopy and linearly growing with height above the canopy at a rate set by the Von Karman constant. Over a flat terrain covered by a uniform canopy, and in the absence of subsidence ($\overline{W}=0$), terms $T_1=T_2=0$ and the mean momentum balance reduces to a balance between turbulent stress gradients and the drag force ($T_3=T_4$). This balance generally defines the so-called 'back-ground' state in flow over hills literature. Conceptually, topographic variability in Eq. (1) is first sensed by perturbations in $\overline{P}$ that result in a non-zero T_2 thereby disrupting the balance between T_3 and T_4 existing on an otherwise flat terrain. The flow responds by accelerating or decelerating (depending on the sign of T_2) thereby resulting in a non-zero T_1. Changes in the vertical gradients in $\overline{U}$ along the longitudinal direction result in a modification of $\partial\overline{u'w'}/\partial z$ often modeled proportional to the gradients in $\bar{U}$ via a turbulent diffusivity as shown in Eq. (2). These topographic variations are now propagated to the main turbulence term T_3 until a new equilibrium is found that also preserves the mean conservation of air mass equation. Eqs. (1) and (2) describe the relation between $\overline{U}$, $\overline{W}$, $\overline{u'w'}$ assuming $\overline{P}$ is known and can be inferred from topographic variations. The determination of $\overline{P}(x,z)$ from topographic variations assumes that the pressure is imposed on the flow and not altered by the flow, a core assumption in analytical models. This assumption was shown to be reasonable for gentle hills (Poggi and Katul, 2007b), the subject here.

Recent flume experiments had shown that the main features of the modeled $\overline{U}$ over a gentle vegetated cosine hill are acceleration on the upwind side and a deceleration on the lee side, both within and above the canopy. Unlike on bare hills or hills with vegetation roughness characterized by a momentum roughness length only, the combined vertical drag force characterizing canopies and the pressure gradients imposed on the wind flow lead to a recirculation region on the lee side of the hill inside the canopy. In this recirculation region, the local $\overline{U}$ reverses direction and flows toward the crest, opposing the regional wind direction established well above the canopy (Finnigan and Belcher, 2004; Poggi and Katul, 2007c). It is these features that lead to 'symmetry breaking' in the mean $\overline{U}$ despite the symmetric nature of the topography.

2.2. Model development

To model seed dispersal on hilly terrain covered with a dense canopy and compare the results for the flat-terrain case, the coupled Eulerian–Lagrangian closure (CELC) approach is employed (e.g. Nathan et al., 2002b; Soons et al., 2004; Nathan and Katul, 2005) with some modifications. The CELC model has two basic modules: the Eulerian module estimates the mean and turbulence wind statistics inside and above a vegetation canopy. These statistics are then used as input into a Lagrangian module, which models stochastic velocities and trajectories of individual seeds until the first-crossing with the ground (Fig. 1). Further movement of the seed by secondary dispersal processes is ignored.

In the Eulerian component, a new first-order analytical model for gentle topography, developed by Poggi et al. (2008, hereafter P08), is used. The model includes minor modifications to an earlier solution by Finnigan and Belcher (2004) to the system of Eqs. (1) and (2). In general, on a vegetated hill, the flow regime is defined by the ratios between the hill half-length, hill height and the canopy density, determining which physical forces are dominant within the canopy and at different heights above the canopy and whether they interact (Poggi et al., 2008). To determine the mean pressure variation across the hill, the analytical models that were developed recently are valid for the simplifying assumptions of gentle hill slope, nearly neutral stability, and deep canopy (i.e. high canopy density), as expressed by the plant area index – the total one sided area of plant parts including stems, branches and foliage, from ground to canopy top, per unit ground surface area ($m^2\,m^{-2}$), hereafter *PAI* (Breda, 2003); and a large drag coefficient (C_d) (Finnigan and Belcher, 2004; Poggi et al., 2008). In this case, the mean pressure variation across the hill is nearly hydrostatic in the vertical and all the longitudinal variation can be described by the topographic variation (Poggi and Katul, 2007b). The linearized analytical model of P08 solves the system of Eqs. (1) and (2) to yield $\overline{U}(x,z)$, $\overline{W}(x,z)$ and $\overline{u'w'}(x,z)$. The model and its solution are described in detail elsewhere (Poggi et al., 2008).

To describe the solution in brief, the modeled main additional driving force of the wind flow over a gentle hill, as compared to a flow on a flat terrain, is the mean pressure gradient (i.e. T_2). The changes in the mean terrain-following wind component ($\overline{U}$) and the normal-to-terrain component ($\overline{W}$) along the hill are modeled as perturbations from the background state, which is the flat-terrain state, and the perturbations in $\overline{U}$ are assumed to be small relatively to the background values. The background horizontal velocity $\vec{U}_b$ is calculated by a simplified analytical model (i.e. $T_3=T_4$) that assumes uniform plant area density (*PAD*) profile. Hence, the only required canopy input parameters are *PAI* and canopy height (H_c). The simple model generates an exponential vertical $\vec{U}_b$ profile inside the canopy and a logarithmic $\vec{U}_b$ profile above the canopy.

Being a first-order closure model, the P08 model does not resolve the higher order statistics such as the velocity variances (Finnigan and Belcher, 2004; Poggi et al., 2008), which are required for the Lagrangian component of CELC. To circumvent this limitation, we assumed that the higher-order statistics are primarily in quasi-local equilibrium with the spatially evolving turbulent stresses near the canopy top. There is some evidence that such an equilibrium assumption for the velocity variances is reasonable inside dense canopies – both from the flume experiments earlier mentioned (Poggi and Katul, 2007a) and from field studies on vineyards situated on sloping terrain (Francone et al., 2012). That is, the vertical variation in the second-order turbulence statistics within the canopy seem to be dominated by the presence of the canopy, while the horizontal variation in turbulence statistics appear to be driven by the spatial variations of $\overline{u'w'}$ just above the canopy top (e.g. see Fig. 5 in Poggi and Katul, 2007a). This latter assumption is known in turbulence research as the moving equilibrium

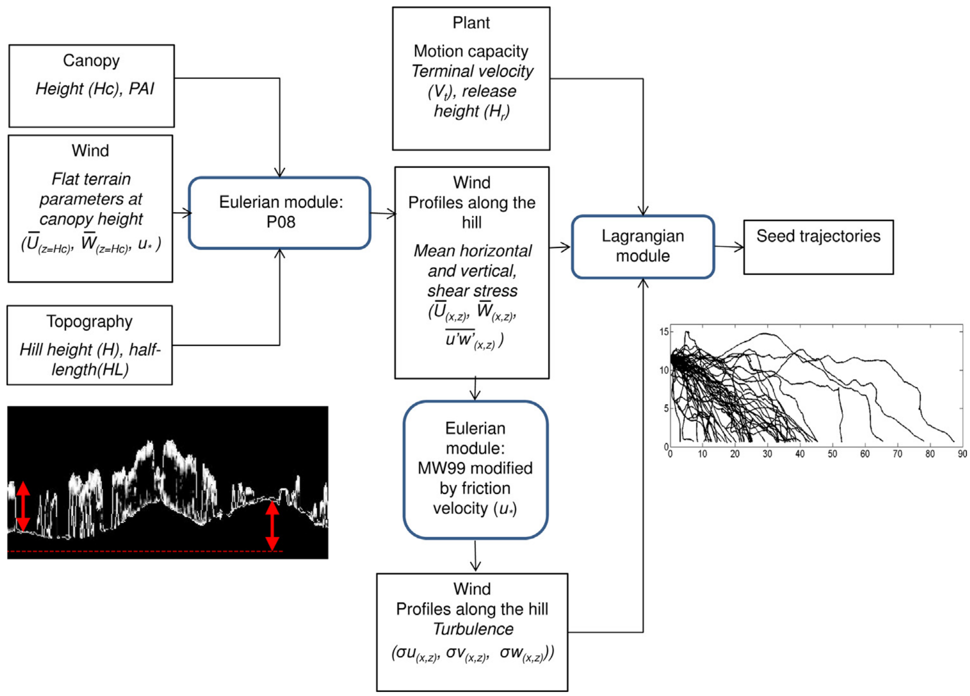

Fig. 1. The flow chart of the mechanistic model for seed dispersal by wind on hilly terrain. Note that the output of the Eulerian module serves as input to the Lagrangian module. P08 stands for the linearized analytical model for wind flow over gentle hills by Poggi et al. (2008). MW99 stands for the second-order closure model for wind over homogeneous surfaces by Massman and Weil (1999). PAI stands for plant area density.

assumption (Kader and Yaglom, 1978). Hence, normalized vertical variations in σ_u/u_*, σ_v/u_*, σ_w/u_* at a given point on the hill surface were modeled as those of the background flat-terrain case using Massman and Weil (1999, hereafter MW99) second-order closure model. Their horizontal variations across the hill were entirely generated by the normalizing variable – the $u_*^2 = -\overline{u'w'}$ at the canopy top as computed by P08. The dissipation rate of the turbulent kinetic energy (ε_c) was also modeled as that derived by MW99, scaled by the local above-canopy u_*, which evolves along the hill.

Next, to model three-dimensional seed trajectories, the two-dimensional wind statistics derived from the simplified analytical Eulerian module were incorporated into the Lagrangian module (Fig. 1) that employs a system of stochastic differential equations to construct synthetic auto-correlated velocity fluctuations in three dimensions at high temporal resolution (on the order of fractions of a second) (see Soons et al., 2004 and Nathan and Katul, 2005 for equations). The statistics of these synthetic fluctuations converge to the values computed from the Eulerian module.

2.3. Model parameterization and setup

In general, the parameters required for the analytical Eulerian module are the hill geometry (hill half-length and height), canopy density structure (drag coefficient C_d, canopy height and *PAI*), the friction velocity at canopy height (u_*) for the background flat-terrain scenario, and its relation with the three turbulence components. To model seed dispersal via the Lagrangian approach, seed motion capacity (*sensu* Nathan et al., 2008a) parameters are also needed (Fig. 1).

The wind, canopy and seed parameters chosen here are for a case study of the dispersal of *P. taeda* in a conspecific stand, parameterized from a well-studied site at Duke Forest, in North Carolina, USA. Additionally, to test for a possible interaction between the topography and the seed motion capacity effects, scenarios with different terminal velocities and release heights were carried out.

2.3.1. Study site

The study site is a *P. taeda* plantation at the Blackwood Division of the Duke Forest (35°97′ N, 79°09′ W) within which there are both flat areas, used for measuring background wind data, and areas of gently sloping topography (see LiDAR image, Fig. 2a).

The study site was the focus of previous studies on canopy structure (e.g. McCarthy et al., 2007), wind flow with forested terrain (e.g. Katul and Chang, 1999) and seed dispersal (e.g. Williams et al., 2006). The stand has well developed understory vegetation, with common broadleaf species including *Liquidambar styraciflua* (sweet gum), *Acer rubrum* (red maple), *Ulmus alata* (winged elm) and *Cornus florida* (flowering dogwood) (McCarthy et al., 2007).

2.3.2. Topography

The hill-geometry parameters needed for the model are the hill height (hereafter *H*) and the hill half-length (defined as half the length from hill crest to hill bottom, hereafter *HL*) in the prevailing wind direction(s). For the seed dispersal simulations, $H/HL = 0.1$ was used, geometrically similar to that in the flume studies employed by P08 to evaluate the performance of the hill wind model, and $H = H_c$.

2.3.3. Canopy

Canopy height value was taken as for the onset of *P. taeda* reproduction, at stand age of 16 years: $H_c = 14.6$ m (Williams et al., 2006). *PAI* was estimated for the peak of the *P. taeda* dispersal season, November (Nathan and Katul, 2005), as $PAI = 3.0$ (based on McCarthy et al., 2007), and uniform *PAD* was assumed as required in the P08 model.

2.3.4. Wind

The normalized turbulence statistics used were according to long-term measurements at the study site (Katul and Chang, 1999, see Table 1). As the main interest here was the general effects of topography-induced changes in the wind field on seed dispersal, $u_* = 1\ \mathrm{m\,s^{-1}}$ was used for the background scenario in all the model

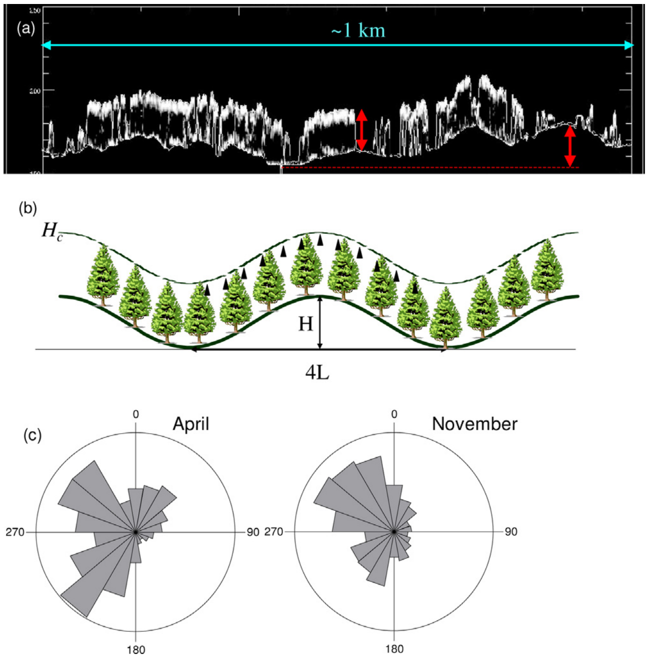

Fig. 2. The gentle hill topography and regional wind directions: (a) topography at the study site, *P. taeda* plantation at one of the divisions at Duke Forest, NC as measured by a LiDAR. Note that hill height is comparable to canopy height (red arrows) and the slope is gentle; (b) topography in the model – the topography is represented as a train of cosine hills, where the length parameters are hill height (H) and hill half-length (HL), with H similar to the canopy height H_c. Black triangles represent the seed release points within the canopy that were used in the dispersal simulations; (c) wind directions distribution during the dispersal season – April and November. Note the bimodality, corresponding to up- and downhill winds.

runs. This u_* value is about 2 times larger than the long-term mean daytime value at the pine site during the dispersal season (Stoy et al., 2006) and hence ensures abscission and possible occurrence of LDD events. The wind direction during the main seed dispersal seasons of *P. taeda* (November) and some of the understory species, e.g. *A. rubrum* (April), is bimodal (Fig. 2c), incorporating both up- and downhill winds.

2.3.5. Spatial setup

In the Eulerian model calculations, the dimension of the spatial domain was set from the ground to $3H_c$ vertically (301 nodes spaced at 0.15 m); and $4HL$ horizontally (601 nodes spaced at 0.97 m). The lateral dimension across the horizontal wind direction (y) is assumed homogenous – constant per x, hence it is unconstrained. In the Lagrangian seed trajectory calculations, a similar domain was used, except for a periodical horizontal dimension (a 'train' of identical hills) and a reflecting top boundary for the vertical dimension so that all seeds released will be contained within the model domain.

Table 1
The description of the hill-canopy system used in the model calculations. Model input variables and their parameterization for the seed dispersal runs are also presented.

Variable	Values
Flat-terrain wind	
Friction velocity (ms^{-1}), u_*	1
Dimensionless standard deviations of velocity components	
Longitudinal, σ_u/u_*	2.3
Lateral, σ_v/u_*	2.1
Vertical, σ_w/u_*	1.3
Topography	
Hill height (m), H	14.6
Hill half length (m), HL	146
Hill height to half length ratio, H/HL	0.1
Canopy	
Canopy height (m), H_c	14.6
Plant area index ($m^2\ m^{-2}$), PAI	3.0
Seed motion capacity	
Terminal velocity ($m\ s^{-1}$), V_t	0.7, 1.0, 1.5
Release height (proportion of canopy height), H_r	0.6, 0.8

2.3.6. Seed attributes

To model seed trajectories via the Lagrangian approach, two seed related input parameters, which are central in determining the motion capacity, are needed: the seed terminal velocity (V_t) and release height (H_r). For V_t, as the focus here is on differences in dispersal kernels resulting from seed release in different spatial contexts, variability of the V_t on the intra-specific level (typically, std = 10–20% of mean V_t, Nathan et al., 2011b) was not represented. Rather, a constant V_t of either 0.7 $m\ s^{-1}$ (the mean of *P. taeda*, Williams et al., 2006), 1 or 1.5 $m\ s^{-1}$ – to approximate typical and higher end values of hardwood species in a nearby forest site (Nathan et al., 2002b) – was used. Seeds with lower V_t are known for trees and other forest plants (e.g. Wright et al., 2008) but are not considered here, since the hill-train geometry assumption becomes much stronger for these seeds that are expected to travel much longer distances (multiple hill wavelengths). For release height, the focus was on releases within the canopy, typical to forested ecosystems (e.g. Nathan et al., 2002b; Wright et al., 2008), with $H_r = 0.8H_c$, as in the 16 year-old *P. taeda* stand (Williams et al., 2006). In addition, for $V_t = 0.7$, release from a lower H_r ($0.6H_c$) was also considered.

For simplicity, random seed abscission was assumed in all the dispersal simulations so as to explore the effects of topography specifically on the seed transport phase of dispersal. Using the model to examine the possible effects of an interaction between non-random seed release and a heterogeneous wind field on dispersal is the next logical step.

2.4. Model evaluation

Before presenting the seed dispersal results for the pine plantation-hill case study, a comparison with the recent flume experiments for a rod canopy on a cosine hill is conducted. This comparison is intended to assess how well the modeled velocity and seed trajectories reproduce kernel measurements in such an idealized system. The dispersal kernels from the experimental releases of spherical artificial seeds at the bottom and the crest of the hill are taken from Katul and Poggi's (2012) flume experiments. For these release locations along the hill, measured and modeled kernels are compared with the model seed and canopy parameters taken similar to those reported in the flume study. The background flat-terrain flow parameters were taken from a separate flume experiment on a similar rod canopy described in Poggi et al. (2004). To mimic the seed release in the flume experiment, which was always an upward ejection from a tube positioned at the canopy top, a minimum instantaneous threshold of $W_{in}(x, z = H_r) = \overline{W_t}(x, z = H_r) + 2|V_t|$ was set on the initial vertical velocity to insure that the fluid vertical velocity is sufficiently large so as to lift the seed from rest inside a stationary tube. In the case of spheres with identical density, a single-valued 'threshold' vertical velocity can be employed. However, the density of these spherical seeds may not be constant, which would have necessitated the use of a probabilistic vertical velocity threshold. This possible variation in the vertical velocity threshold was omitted here. The initial seed vertical velocity was defined as $2W_{in} - V_t$. Furthermore, because seeds are initially released with a vertical acceleration that differs from the surrounding fluid, an exponential relaxation of the seed initial vertical velocity toward the fluid velocity (adjusted by V_t) was also assumed. After this initial relaxation phase, the seed is

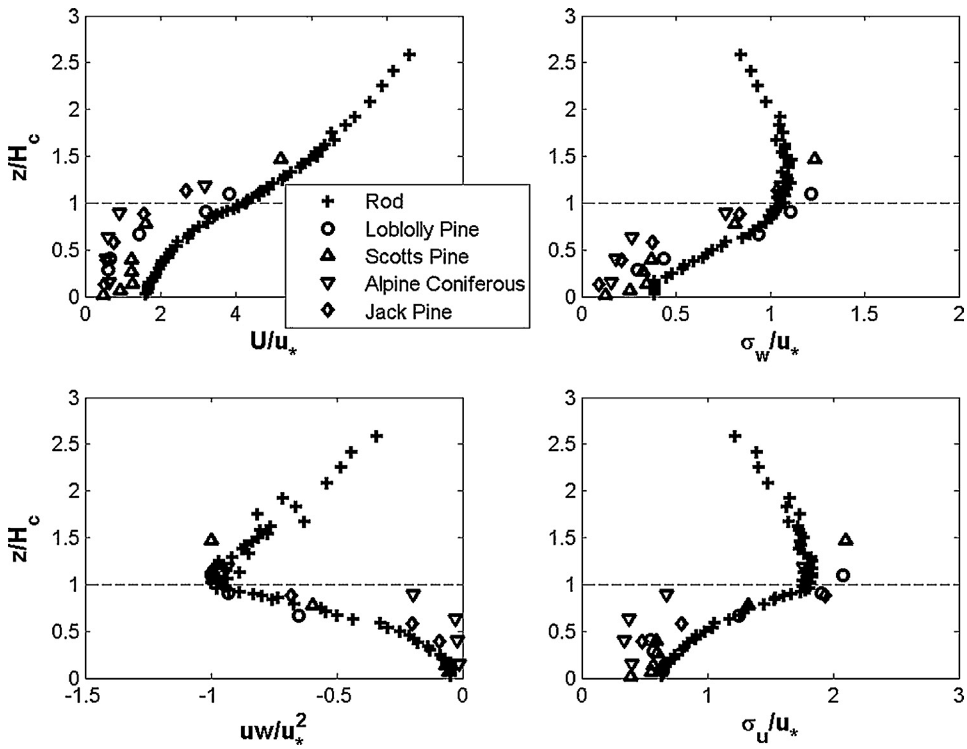

Fig. 3. Comparison between the measured velocity statistics within and above the canopy when normalized by the canopy height (H_c) and friction velocity (u_*) at the canopy top for the dense rod canopy in the flume (H_c = 0.12 m, 1024 rods per m^2), a Loblolly pine forest (H_c = 15 m, *LAI* = 3.5), a Scots Pine forest (H_c = 15 m, *LAI* = 3.0), an Alpine coniferous forest (H_c = 28 m, *LAI* = 4.8), and a Jack pine forest (H_c = 15 m, *LAI* = 2.0): (a) The mean horizontal velocity $\overline{U}$; (b) the mean vertical velocity $\overline{W}$; (c) the shear stress $u'w'$ and (d) the standard deviation of the horizontal component σ_u. The dashed green line represents canopy height.

assumed to have the same acceleration as the moving fluid in the flume. While the canopy system inside the flume is comprised of steel rods within a water medium, it reproduces the main effects of the canopy on the flow statistics – when compared to several types of pine ecosystems as shown in Fig. 3. That is, the density of the rod canopy and its associated drag attenuate the mean flow field in a manner consistent with field experiments conducted inside pine canopies. Hence, the flow field and dispersal trajectories from these flume experiments do represent realistic conditions encountered in tall coniferous forests.

2.5. Seed dispersal simulations

The focus of the dispersal simulations was to examine via model calculations the effect of the release location along the hill on the dispersal pattern. Toward this end, release from the bottom, the crest and from 5 evenly spaced points along the hill on each slope (upwind side and lee side) was modeled as follows: at x = 0, 0.33, . . ., 1.667 of *HL* on each slope (Fig. 2b). This set of model runs was repeated for each of the motion capacity scenarios. The modeled dispersal patterns for the gentle forested hill scenario were compared with those of the corresponding homogenous flat-terrain scenario, which served as a null model.

For each combination of topography scenario, seed release location, and motion capacity, 10^5 trajectories were modeled (overall 3.7×10^6 trajectories). A trajectory run was terminated when the seed reached close to the ground ($z \leq 0.05H_c$), and the dispersal distance was recorded. To compare the model runs for flat and hilly terrain, the median dispersal distance was used as a measure of SDD and the 99th percentile as a measure of LDD. Additionally, the displacement on each axis (x – along the hill, y – across the hill) was recorded and the median displacement along the hill was used to test for the median dispersal direction (MDD) in this dimension. This measure was calculated for all the dispersed seeds and for the 1 percent of seeds that dispersed longest distances.

3. Results

3.1. Modeled wind statistics patterns

As anticipated from previous flume experiments and LES runs, the modeled $\overline{U}$ accelerated on the upwind hill side and decelerated on the lee side. The acceleration and deceleration patterns were asymmetrical, so that the maximal $\overline{U}$ values inside the canopy (where seed release takes place) were at the middle (1*HL*) to the third quarter (1.5*HL*) of the upwind slope, rather than at the crest; and a substantial recirculation region was formed within the canopy on the lee side of the hill, reaching up to $0.75H_c$ in the area adjacent to the middle of the lee slope (Fig. 4a). For the modeled canopy characteristics and hill slope angle, irrespective of the strength of the regional wind, the $\overline{U}$ at canopy top it is expected to be up to 1.5 of that on flat terrain, and higher maximal ratios are expected inside the canopy. The $\overline{W}$ was negative on most of the upwind side and positive at the crest and most of the lee side (Fig. 4b), so that the overall angle of the mean wind vector is not aligned with the topography. The momentum flux ($u'w'$) decreased toward the hill crest, and reached its minimum near the crest on the lee side (Fig. 4c), resulting in modeled minimum in σ_u, σ_v, σ_w there and maximum at the hill bottom (e.g. Fig. 4d).

3.2. Model evaluation

As evidenced by Fig. 5a, for the wind statistics the modeled $\overline{U}$ at the release sites fitted reasonably well the experimental $\overline{U}$ within the canopy at the flume, especially for the hill crest. For the hill bottom, there was some overestimation inside the canopy and underestimation above the canopy. Specifically, the extent of the

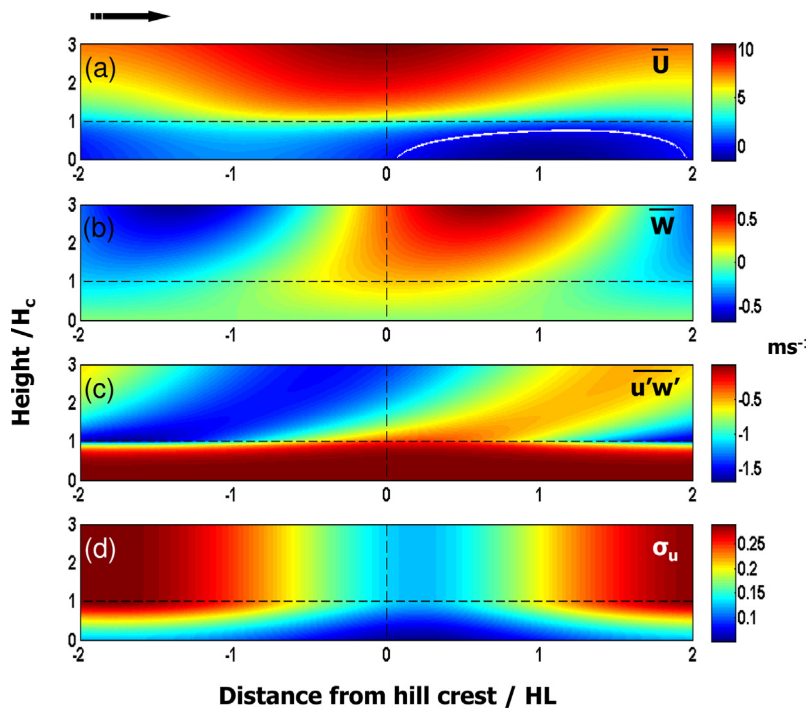

Fig. 4. The spatial trends in the normalized wind statistics along a forested gentle hill as computed by the Eulerian model, shown normalized by the background friction velocity u_*. The parameterization is for the *P. taeda* plantation at Duke Forest and for a hill height to hill half-length ratio of 0.1, as in the seed dispersal simulations. The view here is in terrain-following coordinates so that the ordinate is the height above the hill surface (origin at the hill surface) normalized by canopy height (H_c) and the abscissa is distance across the hill (origin is at hill top), normalized by the hill half-length (*HL*). The canopy height is marked by a dashed horizontal line; the hill crest is marked by a dashed vertical line. The regional wind direction is assumed to be from left to right (black arrow). (a) The mean terrain-following velocity $\overline{U}$, with the upper boundary of the recirculation region marked by the white line; (b) the mean normal-to-terrain velocity; (c) the shear stress $u'w'$ and (d) the standard deviation of the terrain-following component σ_u are shown. The trends for the other normalized variance components are similar.

modeled recirculation region is more restricted and does not reach the hill bottom.

Fig. 5b shows that the modeled dispersal kernels reproduced the main features of the experimental ones: the comparison of the cumulative distribution functions shows that the dispersal distances for seeds released at the hill crest are consistently longer than those for seeds released from hill bottom. Summary statistics show that the mean dispersal distance was higher at the hill crest than at hill bottom (modeled: 0.48 m at hill crest vs. 0.41 m at bottom, 19.7% difference, experiment: 0.52 m vs. 0.37 m accordingly, 40% difference), and the tail of the distribution was heavier (modeled: 4% vs. 1.6% of seeds reaching distances larger than $9H_c$ at crest vs. bottom of the hill, experiment: 10% vs. 4.3% accordingly). The similarity between model and experimental results is viewed as reasonable given the simplifications of the flow field inherent to the model and the uncertainty regarding the exact release mechanism.

3.3. *Modeled seed dispersal patterns on a gentle hill covered with a pine canopy*

Fig. 6 shows that as expected, the variability in the wind flow across the hill affected both the dispersal kernels and the dispersal direction for seeds released at different locations across the hill. For the seeds released on the upwind side, both the modeled median dispersal distances (SDD) and the 99th percentile distances (LDD) were longer than their flat terrain counterparts (see Table A1 for the reference absolute distances on flat terrain), irrespective of motion capacity (V_t and H_r) (Fig. 6a, b, e and f; Fig. A1a and b). The SDD distances for seeds released on the lee side (including hill bottom) almost did not vary with position along the slope and were comparable to those on a flat terrain (0.85–1.25 of flat terrain SDD, Fig. 6a and e; Fig. A1a). The pattern of LDD distances was similar. The maximal distances were always at the middle of the upwind slope for SDD, and at the same location or more toward the crest, at 0.67*HL* (where hill crest = 0*HL*), for LDD, and were considerably (SDD: 1.65–2.05 times, LDD: ~1.5–2.1 times) higher than those on a flat terrain (Fig. 6a, b, e and f, Fig. A1a and b). The median direction of dispersal in the dimension along the hill axis (*x* direction) differed for seed releases at different locations along the hill, and for the LDD-seeds depended additionally on the seed motion capacity parameters. For releases on the upwind side and at hill bottom, the MDD was always in the direction of the regional wind (i.e. toward the crest) similarly to the flat terrain case (Fig. 6c, d, g and h, Fig. A1c and d). For releases on the lee side, the MDD of all seeds was as a rule toward the crest except for seeds released on the upper part of the slope (0.33*HL*), rather than downhill as expected from the direction of the regional wind (Fig. 6c and g). The pattern was different for the seeds that dispersed the longest distances (the 1 top percent of dispersal distances), for which the MDD depended on motion capacity. For seeds released at the higher H_r and having the lower terminal velocity (V_t = 0.7 m s^{-1}), the MDD was in the direction of the regional wind for all release points, while for the higher V_t, or lower H_r at V_t = 0.7 m s^{-1}, the trends were identical to those for all seeds (Fig. 6d and h; Fig. A1d). The latter point will be further elaborated upon in Section 4, via a specific example of dispersion patterns.

4. Discussion

The main novelty here is to utilize a simplified analytical framework for the wind flow field and couple it to a conventional Lagrangian trajectory approach so as to explore the changes introduced by gentle hills on seed dispersal by wind. Agreement between laboratory measurements and model predictions

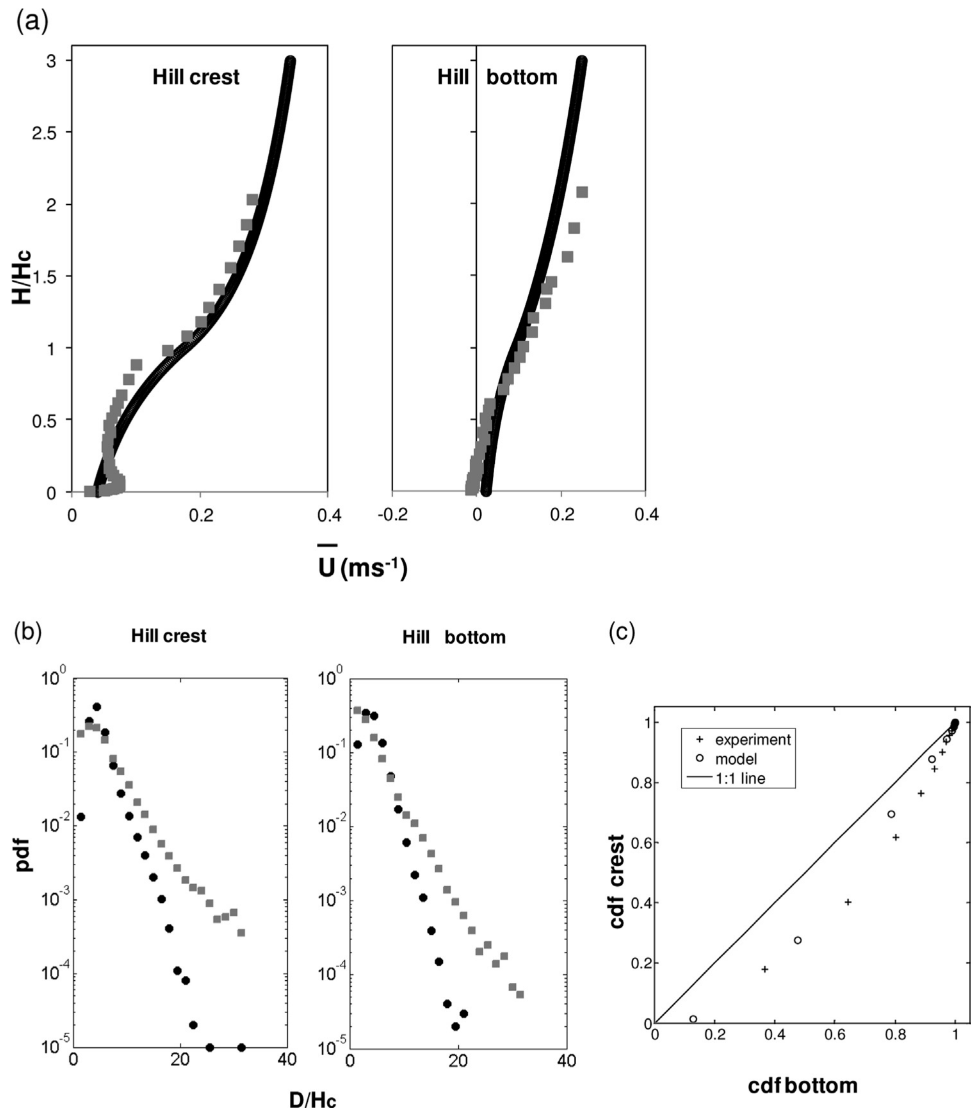

Fig. 5. Model evaluation results for the hill crest vs. hill bottom: (a) The mean terrain-following velocity $\overline{U}$ (modeled: open circles, measured by a laser Doppler anemometry: gray squares), the height (H) is normalized by canopy height (H_c); (b) the modeled seed dispersal kernels (probability of arrival to a specific distance, annotated pdf), as compared to the experimental ones digitized by us (releases from the crest: black circles, releases from the hill bottom: gray squares). The dispersal distances (D) are normalized by H_c. (c) Comparison of the cumulative distribution functions (annotated CDF) of the dispersal distances for releases from the hill crest vs. bottom, for the experiment vs. the model, with 1:1 ratio, as expected on flat terrain, plotted for reference.

provided some confidence in using the model for exploring dispersal patterns within a pine ecosystem situated on hilly terrain.

Regarding the computed dispersal distances, the main finding was that the modeled median dispersal distances (SDD) followed the patterns of the modeled mean terrain-following velocity component ($\overline{U}$) in the vicinity of the release site. This finding is what was hypothesized, where SDD is longer on the upwind side than on flat terrain or the lee side. The trends in the modeled 99th percentile (LDD) distances were overall similar. Notably, the trends were not symmetric between the two slopes. The shift of the SDD dispersal distances relative to those on flat terrain can affect the spatial pattern of post-dispersal processes such as seed predation, further bearing on establishment patterns (Mari et al., 2008; Beckman et al., 2012).

The directionality of dispersal was also considerably different from that on flat terrain. The first outcome from the analysis of the displacement direction is that for a plant located on a hill slope (except for the upper slope), and releasing seeds within a dense canopy, whenever the regional wind is uphill or downhill, the seeds will disperse, at least to short distances, mostly uphill (toward the crest). This is contrary to the flat-terrain scenario, where the majority (e.g., 70–80% in the modeled scenarios) of the seeds dispersed in the direction of the prevailing regional wind and any reversal in direction is only due to turbulence (rather than shift in mean velocity as is the case in hills). This conclusion should be treated with some caution since flume studies did show that the recirculation zone is intermittent (Poggi and Katul, 2007c) so that the modeled proportion of seeds dispersed uphill might be an upper limit here.

For seeds released on the lee side, the main dispersal direction of the LDD seeds is affected by their motion capacity. In the scenario with the highest motion capacity examined ($V_t = 0.7\,\mathrm{m\,s^{-1}}$, $H_r = 0.8$), the median dispersal direction of LDD seeds does follow the direction of the regional wind. A likely explanation has to do with uplifted seeds – i.e., those seeds escaping the canopy. On the lee side, the local direction of $\overline{U}$ above the canopy is aligned downhill with the regional wind direction, unlike the local uphill direction within the canopy (Fig. 3a). Among the seeds released near the recirculation zone, modeled uplifted seeds are expected to disperse mostly downhill. Indeed, on the lee side, out of the

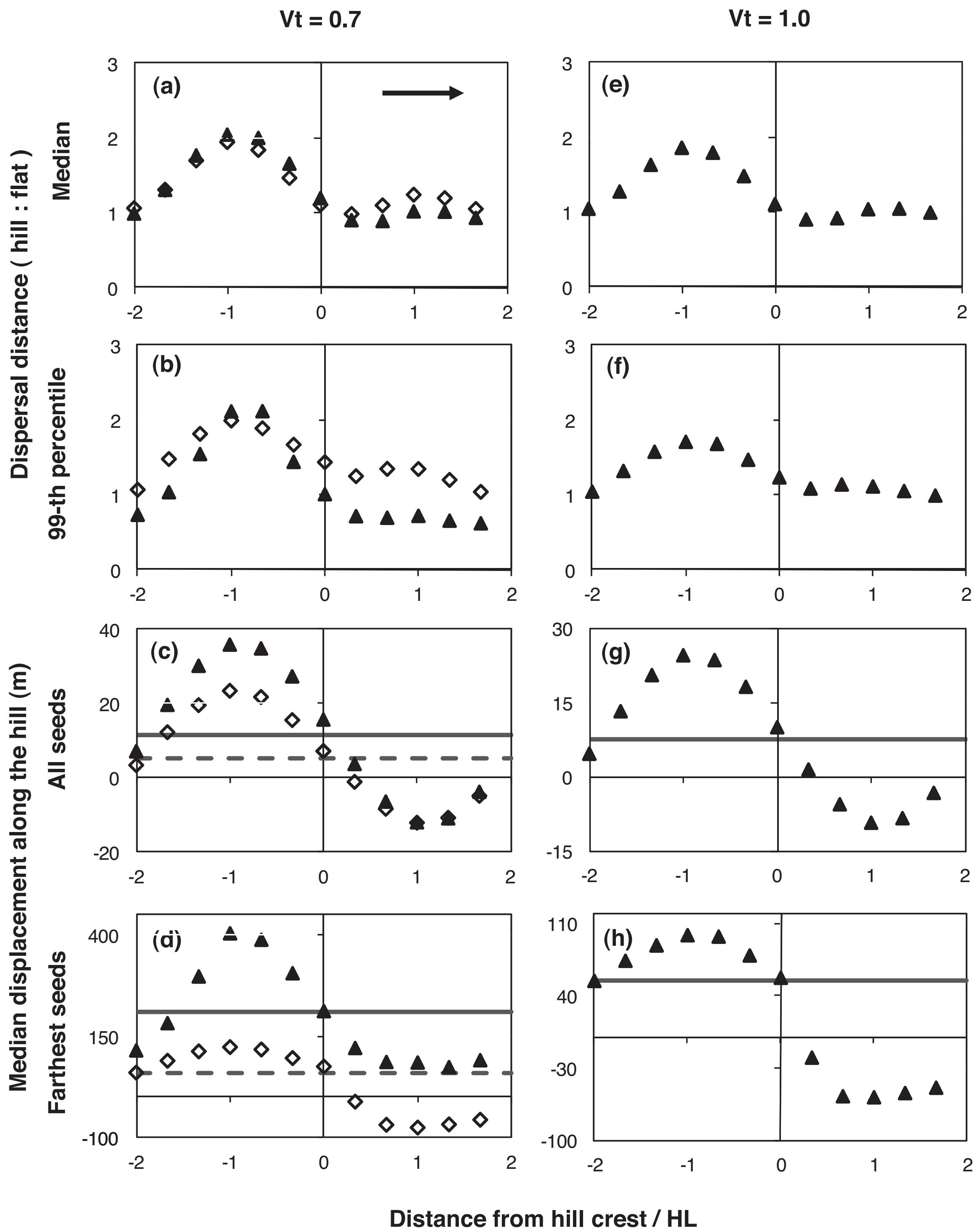

Fig. 6. Dispersal metrics for modeled seed releases at different locations along the hill surface ($x = 0$ is the hill-top, distances are normalized by hill half-length HL) as a function of the seed terminal velocity V_t (a–d): $V_t = 0.7\,\mathrm{m\,s^{-1}}$, (e–h): $V_t = 1\,\mathrm{m\,s^{-1}}$, for seeds released at $H_r = 0.8$ ((a–h) black triangles) or $H_r = 0.6$ ((a–d) open rhombs) of canopy height (H_c). For distances, the hill to flat terrain scenarios ratios for median (a and e), and the 99th percentile (b and f) dispersal distances are shown. For directionality, the median displacement along the hill (MDD) for all seeds (c and g) and for the top 1 percent of seeds with the longest dispersal distances (d and h). Negative MDD values imply dispersal in the direction opposing the regional wind. The values for release on a flat terrain ($H_r = 0.8$: solid line, $H_r = 0.6$: dashed line) are plotted for reference. The arrow in (a) shows the direction of the regional topography-following wind component. At each release point, the statistics for each motion capacity scenario are based on simulation of 10^5 seed trajectories.

seeds moving downhill, 10–270% more seeds were uplifted than non-uplifted (Fig. B1), suggesting that downhill seed motion is associated with uplifting. Furthermore, the proportion of uplifted seeds was in all cases (but one) considerably higher within the LDD seeds than for the rest of the seeds (3.5–46 times higher for specific release points, not shown). This finding corroborates our previous results (Nathan et al., 2002b), yet it should be noted that the heterogeneity in the flow does reduce the occurrence of uplifted seeds. Hence, for the hill scenarios examined here, only in the highest motion-capacity scenario the majority (55–81%) of the LDD seeds

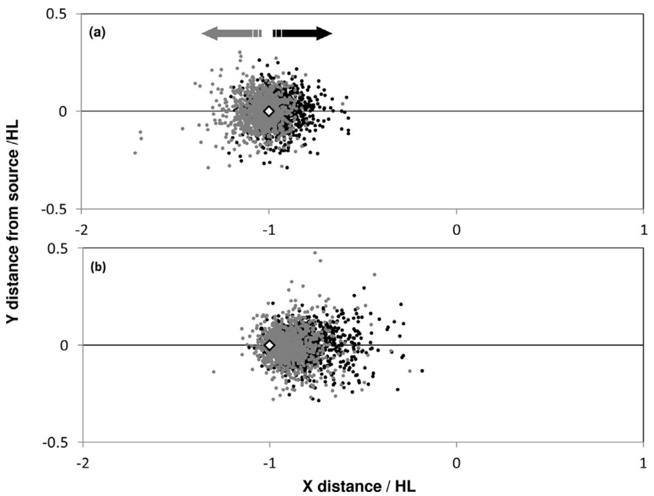

Fig. 7. An example of the effect of topography on dispersal directionality. A map of the seed landing locations for modeled seed releases with opposite regional wind directions: (a) on flat topography (b) on a symmetric cosine hill with 10% slope, release is from mid-slope (all distances are normalized by hill half-length *HL*, for the hill, $X = 0$ is the hill-top). Regional wind direction is marked by arrows, for the hill: black is uphill, gray is downhill. Here seed terminal velocity $V_t = 0.7\ \mathrm{m\,s^{-1}}$, release height $H_r = 0.6$, flat terrain friction velocity $u_* = 1$. The seeds release location is marked by open rhombs. For each wind direction, 10^3 releases were simulated. The *Y* distance is lateral while the *X* is longitudinal.

released on the lee side were uplifted, resulting in median dispersal direction downhill.

The results on dispersal directionality have direct implications for inter-population connectivity. As a rule, the connectivity between adjacent patches is expected to be non-symmetrical and to depend on the prevailing wind directions for wind-dispersed plants. The modeling results imply that on a hill, this asymmetry is expected to be more prominent. To elaborate, consider the scenario of *A. rubrum* growing in Duke Forest on a hillside pine plantation: an understory species with an intermediate motion capacity ($V_t = 0.67\ \mathrm{m\,s^{-1}}$; $H_r = 0.6$), releasing seeds within a dense canopy (Nathan and Katul, 2005). For simplicity, we assume it is experiencing regional winds that are equally likely to occur in the uphill and downhill directions. Because of the recirculation zone, both short and long distance dispersal would be primary upslope, and this population will be better connected with adjacent populations located upslope than with those downslope (for illustration see Fig. 7). For species with high motion capacity, on the other hand, the reversal of dispersal direction found here is expected to affect mostly the local population dynamics (e.g. the inter-sibling distances, impacting sibling competition, see Wright et al., 2008) and not landscape scale processes such as connectivity and population spread. The results on LDD should be again treated with some caution, since the modeling of the turbulence parameters, which strongly impact LDD, was simplified here. At any rate, the anisotropic patterns of seed dispersion found here are not expected to be reflected directly in the distribution patterns of adults. Rather, they are likely to be distorted by post-dispersal processes such as seed predation.

This study also stresses the importance of the vegetation context in which dispersal takes place. First, in sparse canopies on a gentle hill, no recirculation region is expected (Patton and Katul, 2009) and consequently no reversal of dispersal direction is expected on the lee side. Second, the same species might have different motion capacities as a factor of the surrounding vegetation, which strongly influences the release height relative to the vegetation. For example, trees in a population expanding into a shrubland (or other short-canopy vegetation) would have H_r much higher than unity (i.e. releasing seeds well above the vegetation canopy) unlike those dispersing within an established forest. Hence, the trees with higher H_r might not experience the recirculation effects their conspecifics in a forest do. Indeed, a genetic parentage analysis of effective dispersal that was performed on mature trees for a population of Aleppo pine (*Pinus halepensis*) expanding from five source trees within a shrubland, showed substantial dispersal both up- and downhill, in accordance with the predominant regional wind directions (Steinitz et al., 2011).

Thus far, the discussion has focused on a single type of terrain heterogeneity – gentle cosine hills. Recently, Harman and Finnigan (2010) showed that any gentle topographic feature can be spectrally decomposed into a sequence of cosine hills and the analytical solution used here can still be employed for each spectral mode. Hence, the approach proposed here can be extended to arbitrary topographic variation provided the terrain is sufficiently gentle so that pressure perturbations are additive and remain imposed on the mean flow. Thus, the proposed seed dispersal modeling framework can take full advantage of recent remote sensing platforms where canopy height, leaf area index, and ground elevation can be simultaneously measured (Lefsky et al., 2002). It is envisaged that such a framework can provide a first-order estimate of how seeds disperse on complex terrain, thereby serving as a guiding tool to future field experiments aimed at assessing the effects of complex topography on dispersal patterns.

The Eulerian module of the dispersal model can be improved in the future, making use of more elaborate approaches (e.g. higher order closure) to model the wind flow variables. Specifically, for gentle hills, the next step is a more complete modeling of the velocity variance components, possibly by combining different equations for different atmospheric layers (following the discussion in Poggi and Katul, 2008; Poggi et al., 2008). This improved modeling can serve to better predict the LDD patterns across the hill.

More generally, the open challenges for modeling dispersal in hilly terrain are dispersal over steep slopes and over hills covered by heterogeneous canopy. For steep slopes, the effects of topography on the wind flow are expected to be more pronounced. Unlike in the present case, the pressure is expected to be non-hydrostatic and interactive. This interactive effect can be accommodated by adding an additional equation, the mean vertical momentum balance, to the system in Eq. (1). However, this addition prevents analytical tractability and requires far more elaborate numerical solvers to compute the pressure. This is in stark contrast to the case here, where the pressure was completely determined from the hill surface and back-ground friction velocity. It is to be noted that Large Eddy Simulation runs suggest a more wide-spread recirculation zone, possibly extending above the canopy when the topography is quite steep (Dupont et al., 2008). Therefore, a steeper topography might offset some of the effects of a sparse canopy, and consequently a priori hypotheses as to dispersal characteristics in these little explored environments are of little merit. Combining the effects of topography and canopy heterogeneity on the wind flow presents yet another level of complexity, to be resolved in a numerical modeling framework.

To conclude, this study showed that for wind-dispersed species, even gentle topography is expected to introduce considerable variability to dispersal kernels. The model proposed here, enables predictions based on physical principles as to diagnose the effects of location along the hill both on short and on long-distance dispersal. Specifically, dispersal distances are expected to be longer on the upwind side than on flat terrain. Furthermore, the directionality of dispersal is expected to be different from that on flat terrain, bearing both on the local population dynamics and on landscape-scale processes such as inter-population connectivity and population spread. The results further suggest that the effects of topography on dispersal depend on interplay of the seed motion capacity and the surrounding vegetation.

Mechanistic seed dispersal models are increasingly applied in plant population management (Caplat et al., 2012a), such as in estimating spread potential of invasive species or following climate change, and connectivity in fragmented habitats (e.g. Jongejans et al., 2008; Nathan et al., 2011a; Caplat et al., 2012b). Our results show that ignoring even gentle topography in dispersal models may result in considerable bias in the computed dispersal metrics. The modeling approach presented here can be applied for studying the movement over hilly terrain of pollen (Vogler et al., 2009), fungal spores (Norros et al., 2012) and various airborne organisms.

Acknowledgements

This work was supported by Israel Science Foundation grants ISF-474/02, ISF-FIRST 1316/15 and ISF-150/07; and National Science Foundation (NSF) (through NSF-IBN-9981620 and NSF-DEB-0453665). A.T. acknowledges the additional support of Vaadia-BARD Postdoctoral Fellowship Award No. FI-470-2012 from the United States – Israel Binational Agricultural Research and Development (BARD) Fund. R.N. acknowledges the support of Friedrich Wilhelm Bessel Award, Humboldt Foundation; the Minerva Center for Movement Ecology; and Adelina and Massimo Della Pergola Chair of Life Sciences. G.G. K. acknowledges the support from BARD (Award No. IS-4374-11C), the United States Department of Agriculture (USDA #2011-67003-30222), and NSF (NSF-AGS-11-02227). We thank Melissa Chernick for providing us with the tree height and DBH data for *A. rubrum* from the FACE database.

Appendix A. Supplementary data

Supplementary data associated with this article can be found, in the online version, at http://dx.doi.org/10.1016/j.ecolmodel.2013.11.029.

References

Beckman, N.G., Neuhauser, C., Muller-Landau, H.C., 2012. The interacting effects of clumped seed dispersal and distance- and density-dependent mortality on seedling recruitment patterns. J. Ecol. 100, 862–873.
Belcher, S.E., Finnigan, J.J., Harman, I.N., 2008. Flows through forest canopies in complex terrain. Ecol. Appl. 18, 1436–1453.
Belcher, S.E., Harman, I.N., Finnigan, J.J., 2012. The wind in the willows: flows in forest canopies in complex terrain. In: Davis, S.H., Moin, P. (Eds.), Annual Review of Fluid Mechanics, vol. 44, pp. 479–504.
Bohrer, G., Katul, G.G., Nathan, R., Walko, R.L., Avissar, R., 2008. Effects of canopy heterogeneity, seed abscission, and inertia on wind-driven dispersal kernels of tree seeds. J. Ecol. 96, 569–580.
Breda, N.J.J., 2003. Ground-based measurements of leaf area index: a review of methods, instruments and current controversies. J. Exp. Bot. 54, 2403–2417.
Caplat, P., Coutts, S., Buckley, Y.M., 2012a. Modeling population dynamics, landscape structure, and management decisions for controlling the spread of invasive plants. In: Ostfeld, R.S., Schlesinger, W.H. (Eds.), Year in Ecology and Conservation Biology, vol. 1249, pp. 72–83.
Caplat, P., Nathan, R., Buckley, Y.M., 2012b. Seed terminal velocity, wind turbulence, and demography drive the spread of an invasive tree in an analytical model. Ecology 93, 368–377.
Cousens, R., Dytham, C., Law, R., 2008. Dispersal in Plants: A population Perspective. Oxford University Press, Oxford.
Cousens, R.D., Hill, J., French, K., Bishop, I.D., 2010. Towards better prediction of seed dispersal by animals. Funct. Ecol. 24, 1163–1170.
Dupont, S., Brunet, Y., Finnigan, J.J., 2008. Large-eddy simulation of turbulent flow over a forested hill: validation and coherent structure identification. Q. J. R. Meteorol. Soc. 134, 1911–1929.
Finnigan, J.J., Belcher, S.E., 2004. Flow over a hill covered with a plant canopy. Q. J. R. Meteorol. Soc. 130, 1–29.
Francone, C., Katul, G.G., Cassardo, C., Richiardone, R., 2012. Turbulent transport efficiency and the ejection-sweep motion for momentum and heat on sloping terrain covered with vineyards. Agric. For. Meteorol. 162–163, 98–107.
Gugger, P.F., McLachlan, J.S., Manos, P.S., Clark, J.S., 2008. Inferring long-distance dispersal and topographic barriers during post-glacial colonization from the genetic structure of red maple (*Acer rubrum* L.) in New England. J. Biogeogr. 35, 1665–1673.
Harman, I.N., Finnigan, J.J., 2010. Flow over hills covered by a plant canopy: extension to generalised two-dimensional topography. Bound-Layer Meteorol. 135, 51–65.
Horn, S., Raabe, A., Will, H., Tackenberg, O., 2012. TurbSeed—a model for wind dispersal of seeds in turbulent currents based on publicly available climate data. Ecol. Model. 237, 1–10.
Jackson, P.S., Hunt, J.C.R., 1975. Turbulent wind flow over a low hill. Q. J. R. Meteorol. Soc. 101, 929–955.
Jongejans, E., Shea, K., Skarpaas, O., Kelly, D., Sheppard, A.W., Woodburn, T.L., 2008. Dispersal and demography contributions to population spread of *Carduus nutans* in its native and invaded ranges. J. Ecol. 96, 687–697.
Kader, B.A., Yaglom, A.M., 1978. Similarity treatment of moving-equilibrium turbulent boundary layers in adverse pressure-gradients. J. Fluid Mech. 89, 305–342.
Katul, G.G., Chang, W.H., 1999. Principal length scales in second-order closure models for canopy turbulence. J. Clim. Appl. Meteorol. 38, 1631–1643.
Katul, G.G., Poggi, D., 2012. The effects of gentle topographic variation on dispersal kernels of inertial particles. Geophys. Res. Lett. 39, L03401.
Katul, G.G., Porporato, A., Nathan, R., Siqueira, M., Soons, M.B., Poggi, D., Horn, H.S., Levin, S.A., 2005. Mechanistic analytical models for long-distance seed dispersal by wind. Am. Nat. 166, 368–381.
Kuparinen, A., 2006. Mechanistic models for wind dispersal. Trends Plant Sci. 11, 296–301.
Kuparinen, A., Markkanen, T., Riikonen, H., Vesala, T., 2007. Modeling air-mediated dispersal of spores, pollen and seeds in forested areas. Ecol. Model. 208, 177–188.
Lefsky, M.A., Cohen, W.B., Parker, G.G., Harding, D.J., 2002. Lidar remote sensing for ecosystem studies. Bioscience 52, 19–30.
Levey, D.J., Bolker, B.M., Tewksbury, J.J., Sargent, S., Haddad, N.M., 2005. Effects of landscape corridors on seed dispersal by birds. Science 309, 146–148.
Levey, D.J., Tewksbury, J.J., Bolker, B.M., 2008. Modelling long-distance seed dispersal in heterogeneous landscapes. J. Ecol. 96, 599–608.
Levin, S.A., Muller-Landau, H.C., Nathan, R., Chave, J., 2003. The ecology and evolution of seed dispersal: a theoretical perspective. Annu. Rev. Ecol. Evol. Syst. 34, 575–604.
Levine, J.M., Murrell, D.J., 2003. The community-level consequences of seed dispersal patterns. Annu. Rev. Ecol. Evol. Syst. 34, 549–574.
Mack, A.L., 1995. Distance and nonrandomness of seed dispersal by the dwarf casswary *Casuarius bennetti*. Ecography 18, 286–295.
Mari, L., Casagrandi, R., Gatto, M., Avgar, T., Nathan, R., 2008. Movement strategies of seed predators as determinants of plant recruitment patterns. Am. Nat. 172, 694–711.
Massman, W.J., Weil, J.C., 1999. An analytical one-dimensional second-order closure model of turbulence statistics and the Lagrangian time scale within and above plant canopies of arbitrary structure. Bound-Layer Meteorol. 91, 81–107.
McCarthy, H.R., Oren, R., Finzi, A.C., Ellsworth, D.S., Kim, H.-S., Johnsen, K.H., Millar, B., 2007. Temporal dynamics and spatial variability in the enhancement of canopy leaf area under elevated atmospheric CO_2. Glob. Change Biol. 13, 2479–2497.
Nathan, R., Katul, G.G., 2005. Foliage shedding in deciduous forests lifts up long-distance seed dispersal by wind. Proc. Natl. Acad. Sci. U.S.A. 102, 8251–8256.
Nathan, R., Safriel, U.N., Noy-Meir, I., 2001. Field validation and sensitivity analysis of a mechanistic model for tree seed dispersal by wind. Ecology 82, 374–388.
Nathan, R., Horn, H.S., Chave, J., Levin, S.A., 2002a. Mechanistic models for tree seed dispersal by wind in dense forests and open landscapes. In: Levey, D.J., Silva, W.R., Galetti, M. (Eds.), Seed Dispersal and Frugivory: Ecology, Evolution and Conservation. CAB International, Wallingford, UK, pp. 69–82.
Nathan, R., Katul, G.G., Horn, H.S., Thomas, S.M., Oren, R., Avissar, R., Pacala, S.W., Levin, S.A., 2002b. Mechanisms of long-distance dispersal of seeds by wind. Nature 418, 409–413.
Nathan, R., Getz, W.M., Revilla, E., Holyoak, M., Kadmon, R., Saltz, D., Smouse, P.E., 2008a. A movement ecology paradigm for unifying organismal movement research. Proc. Natl. Acad. Sci. U.S.A. 105, 19052–19059.
Nathan, R., Schurr, F.M., Spiegel, O., Steinitz, O., Trakhtenbrot, A., Tsoar, A., 2008b. Mechanisms of long-distance seed dispersal. Trends Ecol. Evol. 23, 638–647.
Nathan, R., Horvitz, N., He, Y., Kuparinen, A., Schurr, F.M., Katul, G.G., 2011a. Spread of North American wind-dispersed trees in future environments. Ecol. Lett. 14, 211–219.
Nathan, R., Katul, G.G., Bohrer, G., Kuparinen, A., Soons, M.B., Thompson, S.E., Trakhtenbrot, A., Horn, H.S., 2011b. Mechanistic models of seed dispersal by wind. Theor. Ecol. 4, 113–132.
Norros, V., Penttila, R., Suominen, M., Ovaskainen, O., 2012. Dispersal may limit the occurrence of specialist wood decay fungi already at small spatial scales. Oikos 121, 961–974.
Nuttle, T., Haefner, J.W., 2005. Seed dispersal in heterogeneous environments: bridging the gap between mechanistic dispersal and forest dynamics models. Am. Nat. 165, 336–349.
Ozinga, W.A., Bekker, R.M., Schaminee, J.H.J., Van Groenendael, J.M., 2004. Dispersal potential in plant communities depends on environmental conditions. J. Ecol. 92, 767–777.
Patton, E.G., Katul, G.G., 2009. Turbulent pressure and velocity perturbations induced by gentle hills covered with sparse and dense canopies. Bound-Layer Meteor. 133, 189–217.
Poggi, D., Katul, G., 2007a. The ejection-sweep cycle over bare and forested gentle hills: a laboratory experiment. Bound-Layer Meteor. 122, 493–515.
Poggi, D., Katul, G.G., 2007b. An experimental investigation of the mean momentum budget inside dense canopies on narrow gentle hilly terrain. Agric. For. Meteorol. 144, 1–13.

Poggi, D., Katul, G.G., 2007c. Turbulent flows on forested hilly terrain: the recirculation region. Q. J. R. Meteorol. Soc. 133, 1027–1039.
Poggi, D., Katul, G.G., 2008. Turbulent intensities and velocity spectra for bare and forested gentle hills: flume experiments. Bound-Layer Meteorol. 129, 25–46.
Poggi, D., Porporato, A., Ridolfi, L., Albertson, J.D., Katul, G.G., 2004. The effect of vegetation density on canopy sub-layer turbulence. Bound-Layer Meteorol. 111, 565–587.
Poggi, D., Katul, G.G., Finnigan, J.J., Belcher, S.E., 2008. Analytical models for the mean flow inside dense canopies on gentle hilly terrain. Q. J. R. Meteorol. Soc. 134, 1095–1112.
Reader, R.J., Buck, J., 1986. Topographic variation in the abundance of *Hieracium floribundum*—relative importance of differential seed dispersal, seedling establishment, plant survival and reproduction. J. Ecol. 74, 815–822.
Ridley, H.N., 1930. The Dispersal of Plants throughout the World. Reeve, Ashford.
Rupp, T.S., Chapin, F.S., Starfield, A.M., 2001. Modeling the influence of topographic barriers on treeline advance at the forest-tundra ecotone in northwestern Alaska. Clim. Change 48, 399–416.
Soons, M.B., Heil, G.W., Nathan, R., Katul, G.G., 2004. Determinants of long-distance seed dispersal by wind in grasslands. Ecology 85, 3056–3068.
Steinitz, O., Troupin, D., Vendramin, G.G., Nathan, R., 2011. Genetic evidence for a Janzen-Connell recruitment pattern in reproductive offspring of *Pinus halepensis* trees. Mol. Ecol. 20, 4152–4164.
Stoy, P.C., Katul, G.G., Siqueira, M.B.S., Juang, J.-Y., Novick, K.A., Uebelherr, J.M., Oren, R., 2006. An evaluation of models for partitioning eddy covariance-measured net ecosystem exchange into photosynthesis and respiration. Agric. For. Meteorol. 141, 2–18.
Stull, R.B., 1988. An Introduction to Boundary-Layer Meteorology. Kluwer Academic Publishers, Dordrecht.
Tackenberg, O., 2003. Modeling long distance dispersal of plant diaspores by wind. Ecol. Monogr. 73, 173–189.
Trakhtenbrot, A., Nathan, R., Perry, G., Richardson, D.M., 2005. The importance of long-distance dispersal in biodiversity conservation. Divers. Distrib. 11, 173–181.
van der Pijl, L., 1982. Principles of Dispersal in Higher Plants, 3rd ed. Springer, Berlin.
Vogler, A., Eisenbeiss, H., Aulinger-Leipner, I., Stamp, P., 2009. Impact of topography on cross-pollination in maize (*Zea mays* L.). Eur. J. Agron. 31, 99–102.
Williams, C.G., LaDeau, S.L., Oren, R., Katul, G.G., 2006. Modeling seed dispersal distances: implications for transgenic *Pinus taeda*. Ecol. Appl. 16, 117–124.
Willson, M.F., Rice, B.L., Westoby, M., 1990. Seed dispersal spectra—a comparison of temperate plant-communities. J. Veg. Sci. 1, 547–562.
Wright, S.J., Trakhtenbrot, A., Bohrer, G., Detto, M., Katul, G.G., Horvitz, N., Muller-Landau, H.C., Jones, F.A., Nathan, R., 2008. Understanding strategies for seed dispersal by wind under contrasting atmospheric conditions. Proc. Natl. Acad. Sci. U.S.A. 105, 19084–19089.